Inorg. Chem. **2004**, *43*, 4464–4470

New Halide-Centered Discrete Ag^{I}_{8} Cubic Clusters Containing Diselenophosphate Ligands, $\{Ag_8(X)[Se_2P(OR)_2]_6\}(PF_6)$ (X = Cl, Br; R = Et, Pr, ^{i}Pr): Syntheses, Structures, and DFT Calculations

C. W. Liu,* Hsien-Chung Haia, Chiu-Mine Hung, Bidyut Kumar Santra, and Ben-Jie Liaw

Department of Chemistry, Chung Yuan Christian University, Chung-Li, Taiwan 320, R.O.C.

Zhenyang Lin*

Department of Chemistry, The Hong Kong University of Science & Technology, Clear Water Bay, Kowloon, Hong Kong

Ju-Chun Wang

Department of Chemistry, Soochow University, Taipei, Taiwan 111, R.O.C.

Received April 9, 2004

Six clusters $Ag_8(\mu_8\text{-}X)[Se_2P(OR)_2]_6(PF_6)$ (R = Et, X = Cl, **1a**, X = Br, **1b**; R = Pr, X = Cl, **2a**, X = Br, **2b**; R = ^{i}Pr, X = Cl, **3a**, X = Br, **3b**) were isolated from the reaction of $[Ag(CH_3CN)_4](PF_6)$, $NH_4[Se_2P(OR)_2]$, and Bu_4NX in a molar ratio of 4:3:1 in CH_2X_2. Positive FAB mass spectra show *m*/*z* peaks at 2573.2 for **1a**, 2617.3 for **1b**, 2740.9 for **2a**, 2786.9 for **2b**, 2742.3 for **3a**, and 2787.0 for **3b** due to respective molecular cation, $(M - PF_6)^+$. ^{31}P NMR spectra of **1a**–**3b** display a singlet at δ 82.3, 81.5, 82.9, 81.7, 76.3, and 75.8 ppm with a set of satellites (J_{PSe} = 661, 664, 652, 652, 656, and 656 Hz, respectively). The X-ray structure (**1a**–**2b**) consists of a discrete cationic cluster in which eight silver ions are linked by six diselenophosphate ligands and a central μ_8-Cl or μ_8-Br ion with a noncoordinating PF_6^- anion. The shape of the molecule is a halide-centered distorted Ag_8 cubic cluster. The dsep ligand exhibits a tetrametallic tetraconnective (μ_2, μ_2) coordination pattern, and each caps on a square face of the cube. Each silver atom of the cube is coordinated by three selenium atoms and the central chloride or bromide ion. Additionally, molecular orbital calculations at the B3LYP level of the density functional theory have been carried out to study the Ag–μ_8–X (X = Cl, Br) interactions for cluster cations $[Ag_8(\mu_8\text{-}X)\{Se_2P(OR)_2\}_6]^+$. Calculations show very weak bonding interactions exist between μ_8-X and Ag atoms of the cube.

Introduction

The coordination chemistry of anions has received much attention because of the realization of the important roles that anions play in biology, medicine, catalysis, and the environment.[1] Interest has been shown in using anions to direct self-assembly processes[2] and as templates[3] in the area of supramolecular chemistry. The halide ions are mostly studied because of their variable coordination modes, and the coordination polyhedra for the halides are planar,[4] tetrahedral,[5] octahedral,[6] and cubic.[7]

Molecular cubic clusters encapsulating halide ion are interesting in view of their unusual bonding characteristics.[8]

* To whom correspondence should be addressed. E-mail:chenwei@cycu.edu.tw (C.W.L.).

(1) (a) Bondy, C. R.; Loeb, S. J. *Coord. Chem. Rev.* **2003**, *240*, 77. (b) Beer, P. D.; Gale, P. A. *Angew. Chem., Int. Ed.* **2001**, *40*, 486. (c) Gale, P. A. *Coord. Chem. Rev.* **2000**, *199*, 181.

(2) (a) Hossain, Md. A.; Llinares, J.; Powell, D.; Bowman-James, K. *Inorg. Chem.* **2001**, *40*, 2936. (b) Seel, C.; Vögtle, F. *Chem. Eur. J.* **2000**, *6*, 21. (c) Campos-Fernandez, C. S.; Clerac, R.; Dunbar, K. R. *Angew. Chem., Int. Ed.* **1999**, *38*, 3477. (d) Vilar, R.; Mingos, D. M. P.; White, A. J. P.; Williams, D. J. *Angew. Chem., Int. Ed.* **1998**, *37*, 1258. (e) Fleming, J. S.; Mann, K. L. V.; Carraz, C.-A.; Psillakis, E.; Jeffery, J. C.; McCleverty, J. A.; Ward, M. D. *Angew. Chem., Int. Ed.* **1998**, *37*, 1279. (f) Fender, N. S.; Kahwa, I. A.; White, A. J. P.; Williams, D. J. *J. Chem. Soc., Dalton Trans.* **1998**, 1729. (g) Fyfe, M. C. T.; Glink, P. T.; Menzer, S.; Stoddart, J. F.; White, A. J. P.; Williams, D. J. *Angew. Chem., Int. Ed.* **1997**, *36*, 2068. (h) Hasenknopf, B.; Lehn, J.-M.; Boumediene, N.; Dupont-Gervais, A.; Van Dorsselaer, A.; Kneisel, B.; Fenske, D. *J. Am. Chem. Soc.* **1997**, *119*, 10956.

10.1021/ic049533p CCC: $27.50
Published on Web 06/08/2004

Although several halide-centered cubic copper clusters that are mixed-valence, $Cu^{II}_6Cu^I_8(\mu_8\text{-Cl})L_{12}$,[9] discrete, $\{Cu^I_8(\mu_8\text{-X})L_6\}^+$ (X = Cl, Br),[7d,10] and polymeric, $\{[Cu^I_8(Cl)L_6]Cl\}_\infty$,[11] are known in the literature, a cuboidal silver cluster with a halide in its center is extremely rare. Birker reported first a mixed-metal cluster, $[Ni^{II}_6Ag^I_8(D\text{-pen})_{12}Cl]$,[5−12] whose central core can be envisaged with eight silver atoms arranged in the corner of the cube with the chloride in its center. Recently, Mingos and co-workers reported several tetradecanuclear silver cages, $[Ag_{14}(C{\equiv}C^tBu)_{12}X]Y$ (X = F, Cl, Br; Y = OH, BF_4),[13] whose central portion is also a cubic array of silver atoms with a halide ion in the center of the cube, and the stabilization of these compounds is also attributed to the argentophilic Ag···Ag interaction.[14] A preliminary account of our results containing halide-centered cubic silver clusters, $\{Ag_8(X)[Se_2P(OEt)_2]_6\}(PF_6)$ (X = Cl, Br), which indeed include the first halide-centered discrete Ag^I_8 cube, has been communicated.[15] Herein, we report the detailed syntheses and characterizations of halide-centered discrete Ag^I_8 cubic clusters, $\{Ag_8(\mu_8\text{-X})[Se_2P(OR)_2]_6(PF_6)\}$(R = Et, Pr, ^{i}Pr; X = Cl, Br). In addition, the nature of Ag−μ_8-X bonding interactions of these clusters has been studied by molecular orbital calculations at the B3LYP level of the density functional theory.

Experimental Section

Materials and Measurements. All chemicals were purchased from commercial sources and used as received. Commercial CH_2Cl_2 and ROH were distilled from P_4O_{10} and Mg, respectively. Hexane and diethyl ether were distilled from Na/K. All the reactions were performed in oven-dried Schlenk glassware by using standard inert-atmosphere techniques. The starting silver(I) complexes, $Ag(CH_3CN)_4(PF_6)$[16] and the ligands, $NH_4Se_2P(OR)_2$ (R= Et, Pr, ^{i}Pr),[17] were prepared according to the literature methods. The elemental analyses were done using a Perkin-Elmer 2400 CHN analyzer. NMR spectra were recorded on Bruker AC-F200 and Advance-300 Fourier transform spectrometers. The $^{31}P\{^1H\}$ NMR is referenced externally against 85% H_3PO_4 ($\delta = 0$). Positive FAB mass spectra were carried out on a VG 70-250S mass spectrometer with nitrobenzyl alcohol as the matrix.

Preparation of $Ag_8(\mu_8\text{-X})[Se_2P(OR)_2]_6(PF_6)$ (R = Et, X = Cl, 1a, X = Br, 1b; R = Pr, X = Cl, 2a, X = Br, 2b; R = ^{i}Pr, X = Cl, 3a, X = Br, 3b). Compounds **1a**−**3b** were prepared by following a general procedure using respective halo-solvents (CH_2X_2) and tetrabutylammonium halide. A representative, detailed procedure is given for **1a**. Dichloromethane (50 mL) was added to a Schlenk flask (100 mL) containing $[Ag(CH_3CN)_4](PF_6)$ (1.668, 4 mmol), $NH_4[Se_2P(OEt)_2]$ (0.90 g, 3 mmol), and Bu_4NCl (0.278 g, 1 mmol). The solution mixture was stirred for 24 h at 0 °C under a dinitrogen atmosphere. The solution color changed from colorless to brown during the reaction period, and some AgCl precipitates were formed. The solvent was evaporated under vacuum. Then, it was extracted with ether (100 mL) to afford a yellow solution and brown precipitate. The brown precipitate was washed with copious amounts of methanol which yielded the pure, white compound $Ag_8(\mu_8\text{-Cl})[Se_2P(OEt)_2]_6(PF_6)$, **1a**, in 55% yield. Solvent was removed by rotary evaporation from the yellow ether extract which afforded $Ag_{10}(\mu_{10}\text{-Se})[Se_2P(OEt)_2]_8$ in ∼20% yield. This Ag_{10} cluster is known to form in the reaction of $[Ag(CH_3CN)_4](PF_6)$ and $NH_4[Se_2P(OR)_2]$ in diethyl ether medium[17b] in the absence of halide ions.

Compound 1a. (Yield ∼55%, 0.747 g.) Anal. Calcd for $C_{24}H_{60}ClAg_8F_6O_{12}P_7Se_{12}$: C, 10.61; H, 2.21. Found: C, 11.13; H, 2.26. FAB MS, *m*/*z* 2573.2 (M^+). ^1H NMR ($CDCl_3$) δ 1.39 [t, 36H, OCH_2CH_3, $^3J_{HH}$ = 7 Hz], 4.17 [m, 24H, OCH_2CH_3]; $^{31}P\{^1H\}$ NMR ($CDCl_3$) δ 82.3 [s, 6P, $P(OR)_2$, J_{PSe} = 661 Hz], −143.0 (septet, PF_6^-, J_{PF} = 712).

Compound 1b. (Yield ∼61%, 0.869 g.) Anal. Calcd for $C_{24}H_{60}BrAg_8F_6O_{12}P_7Se_{12}\cdot C_6H_{14}$: C, 12.64; H, 2.60. Found: C, 12.67; H, 2.15. FAB MS, *m*/*z* 2617.3 (M^+). ^1H NMR ($CDCl_3$) δ 1.39 [t, 36H, OCH_2CH_3, $^3J_{HH}$ = 7 Hz], 4.17 [m, 24H, OCH_2CH_3]; $^{31}P\{^1H\}$

(3) (a) Sessler, J. L.; Sansom, P. I.; Andrievsky, A.; Gale, P. A.; Lynch, V. *Angew. Chem., Int. Ed. Engl.* **1996**, *35*, 2782. (b) Zheng, Z.; Knobler, C. B.; Hawthorne, M. F. *J. Am. Chem. Soc.* **1995**, *117*, 5105. (c) Yang, X.; Knobler, C. B.; Zheng, Z.; Hawthorne, M. F. *J. Am. Chem. Soc.* **1994**, *116*, 7142. (d) Salta, J.; Chen, Q.; Chang, Y.; Zubieta, J. *Angew. Chem., Int. Ed. Engl.* **1994**, *33*, 757. (e) Sessler, J. L.; Mody, T. D.; Lynch, V. *J. Am. Chem. Soc.* **1993**, *115*, 3346. (f) Müller, A.; Rohlfing, R.; Krickemeyer, E.; Penk, M.; Bögge, H. *Angew. Chem., Int. Ed. Engl.* **1993**, *32*, 909.

(4) (a) Wang, R.; Selby, H. D.; Liu, H.; Carducci, M. D.; Jin, T.; Zhang, Z.; Anthis, J. W.; Staples, R. J. *Inorg. Chem.* **2002**, *41*, 278. (b) Wang, R.; Jin, T.; Zhang, Z.; Staples, R. J. *Angew. Chem., Int. Ed.* **1999**, *38*, 1813. (c) Yang, X.; Knobler, C. B.; Hawthorne, M. F. *Angew. Chem., Int. Ed. Engl.* **1991**, *11*, 1507.

(5) (a) Gonzalez-Duarte, P.; Clegg, W.; Casals, I.; Sola, J.; Rius, J. *J. Am. Chem. Soc.* **1998**, *120*, 1260. (b) Dance, I. G. *Aust. J. Chem.* **1985**, *38*, 1391.

(6) (a) Lee, H.; Knobler, C. B.; Hawthorne, M. F. *J. Am. Chem. Soc.* **2001**, *123*, 3148. (b) Krautscheid, H.; Lode, C.; Vielsack, F.; Vollmer, H. *J. Chem. Soc., Dalton Trans.* **2001**, 1099. (c) Lee, H.; Knobler, C. B.; Hawthorne, M. F. *Angew. Chem., Int. Ed.* **2000**, *39*, 776. (d) Wang, Q.-M.; Mak, T. C. W. *Chem. Commun.* **2000**, 1435.

(7) (a) Fackler, J. P., Jr.; Staples, R. J.; Liu, C. W.; Stubbs, R. T.; Lopez, C.; Pitts, J. T. *Pure Appl. Chem.* **1998**, *70*, 839. (b) Burgi, H. B.; Gehrer, H.; Strickler, P.; Winkler, F. K. *Helv. Chim. Acta* **1976**, *59*, 2558. (c) Dance, I. G.; Garbutt, R.; Craig, D. *Inorg. Chem.* **1987**, *26*, 3732. (d) Fackler, J. P., Jr. *Inorg. Chem.* **2002**, *41*, 6959. (e) Degroot, M. W.; Corrigan, J. F. In *Comprehensive Coordination Chemistry II*; McCleverty, J. A., Meyer, T. J., Eds.; Pergamon: London, 2004; Vol. 7, p 57.

(8) Garland, M. T.; Halet, J.-F.; Saillard, J.-Y. *Inorg. Chem.* **2001**, *40*, 3342.

(9) (a) Schugar, H. J.; Ou, C.-C.; Thich, J. A.; Potenza, J. A.; Felthouse, T. R.; Haddad, M. S.; Hendrickson, D. N.; Furey, W., Jr.; Lalancette, R. A. *Inorg. Chem.* **1980**, *19*, 543. (b) Birker, P. J. M. W. L. *Inorg. Chem.* **1979**, *18*, 3502. (c) Birker, P. J. M. W. L.; Freeman, H. C. *J. Am. Chem. Soc.* **1977**, *99*, 6890. (d) Birker, P. J. M. W. L.; Freeman, H. C. *J. Chem. Soc., Chem. Commun.* **1976**, 312. (e) Schugar, H. J.; Ou, C.-C.; Thich, J. A.; Lalancette, R. A.; Furey, W., Jr. *J. Am. Chem. Soc.* **1976**, *98*, 3047.

(10) (a) Liu, C. W.; Hung, C.-M.; Chen, H.-C.; Wang, J.-C.; Keng, T.-C.; Guo, K. *Chem. Commun.* **2000**, 1897. (b) Liu, C. W.; Hung, C.-M.; Santra, B. K.; Chen, H.-C.; Hsueh, H.-H.; Wang, J.-C. *Inorg. Chem.* **2003**, *42*, 3216.

(11) Wu, D.; Huang, J.-Q.; Lin, Y.; Haung, J.-L. *Sci. Sin., Ser. B. (Engl. Ed)* **1988**, *31*, 800.

(12) (a) Birker, P. J. M. W. L.; Reedijk, J.; Verschoor, G. C. *Inorg. Chem.* **1981**, *20*, 2877. (b) Birker, P. J. M. W. L. *J. Chem. Soc., Chem. Commun.* **1980**, 946.

(13) (a) Rais, D.; Yau, J.; Mingos, D. M. P.; Vilar, R,; White, A. J. P.; Williams, D. J. *Angew. Chem., Int. Ed.* **2001**, *40*, 3464. (b) Rais, D.; Mingos, D. M. P.; Vilar, R.; White, A. J. P.; Williams, D. J. *J. Organomet. Chem.* **2002**, *652*, 87.

(14) (a) Che, C.-M.; Tse, M.-C.; Chan, M. C. W.; Cheung, K.-K.; Philips, D. L.; Leung, K.-H. *J. Am. Chem. Soc.* **2000**, *122*, 2464. (b) Rawashdeh-Omary, M. A.; Patterson, H. H. *J. Am. Chem. Soc.* **2000**, *122*, 10371. (c) Omary, M. A.; Webb, T. R.; Assefa, Z.; Shankle, G. E.; Patterson, H. H. *Inorg. Chem*, **1998**, *37*, 1380. (d) Wang, Q.-M.; Mak, T. C. W. *Angew. Chem., Int. Ed.* **2002**, *41*, 4135. (e) Guo, G.-C.; Mak, T. C. W. *Angew. Chem., Int. Ed.* **1998**, *37*, 3183.

(15) Liu, C. W.; Hung, C.-M.; Haia, H.-C.; Liaw, B.-J.; Liou, L.-S.; Tsai, Y.-F.; Wang, J.-C. *Chem. Commun.* **2003**, 976.

(16) Nelsson, K.; Oskarsson, A. *Acta Chem. Scand., Ser. A* **1984**, *38*, 79.

(17) (a) Kudchadker, M. V.; Zingaro, R. A.; Irgolic, K. J. *Can. J. Chem.* **1968**, *46*, 1415. (b) Liu, C. W.; Shang, I.-J.; Hung, C.-M.; Wang, J.-C.; Keng, T.-C. *J. Chem. Soc., Dalton. Trans.* **2002**, 1974.

NMR ($CDCl_3$) δ 81.5 [s, 6P, $P(OR)_2$, J_{PSe} = 664 Hz], −143.0 (septet, PF_6^-, J_{PF} = 712).

Compound 2a. (Yield ~41%, 0.590 g.) Anal. Calcd for $C_{36}H_{84}ClAg_8F_6O_{12}P_7Se_{12}$: C, 14.97; H, 2.91. Found: 14.40; H, 2.77. FAB MS, *m*/*z* 2740.9 (M^+). ^{1}H NMR ($CDCl_3$) δ 0.98 (t, 36H, $OCH_2CH_2CH_3$), 1.74 [m, 24H, $OCH_2CH_2CH_3$], 4.05 [m, 24H, $OCH_2CH_2CH_3$]; ^{31}P {^{1}H} NMR ($CDCl_3$) δ 82.9 [s, 6P, $P(OR)_2$, J_{PSe} = 652 Hz], −143.0 (septet, PF_6^-, J_{PF} = 712).

Compound 2b. (Yield ~51, 0.747 g.) Anal. Calcd for $C_{36}H_{84}BrAg_8F_6O_{12}P_7Se_{12}$: C, 14.74; H, 2.87. Found: 14.85; H, 3.10. FAB MS, *m*/*z* 2786.9 (M^+). ^{1}H NMR ($CDCl_3$) δ 0.99 (t, 36H, $OCH_2CH_2CH_3$), 1.77 [m, 24H, $OCH_2CH_2CH_3$], 4.05 [m, 24H, $OCH_2CH_2CH_3$]; ^{31}P {^{1}H} NMR ($CDCl_3$) δ 81.7 [s, 6P, $P(OR)_2$, J_{PSe} = 652 Hz], −143.0 (septet, PF_6^-, J_{PF} = 712).

Compound 3a. (Yield ~68%, 0.981 g.) Anal. Calcd for $C_{36}H_{84}ClAg_8F_6O_{12}P_7Se_{12}$: C, 14.97; H, 2.91. Found: C, 14.80; H, 2.80. FAB MS, *m*/*z* 2742.3 (M^+). ^{1}H NMR ($CDCl_3$) δ 1.36 [d, 72H, $OCH(CH_3)_2$, $^3J_{HH}$ = 6 Hz], 4.78 [m, 12H, $OCH(CH_3)_2$]; ^{31}P {^{1}H} NMR ($CDCl_3$) δ 76.3 [s, 6P, $P(OR)_2$, J_{PSe} = 656 Hz], −143.0 (septet, PF_6^-, J_{PF} = 712).

Compound 3b. (Yield ~65%, 0.952 g.) Anal. Calcd for $C_{36}H_{84}BrAg_8F_6O_{12}P_7Se_{12}$: C, 14.74; H, 2.87. Found: C, 14.40; H, 2.83. FAB MS, *m*/*z* 2787.0 (M^+). ^{1}H NMR ($CDCl_3$) δ 1.40 [d, 72H, $OCH(CH_3)_2$, $^3J_{HH}$ = 6 Hz], 4.86 [m, 12H, $OCH(CH_3)_2$]; ^{31}P {^{1}H} NMR ($CDCl_3$) δ 75.8 [s, 6P, $P(OR)_2$, J_{PSe} = 656 Hz], −143.0 (septet, PF_6^-, J_{PF} = 712).

Safety Note. *Selenium and its derivatives are toxic! These materials should be handled with great caution.*

X-ray Crystallographic Procedures. The structures of **1a**, **1b**, **2a**, and **2b** were obtained by the single-crystal X-ray diffraction technique. Crystals were mounted on the tips of glass fibers with epoxy resin. Data were collected on a Siemens SMART CCD (charged coupled device) diffractometer for compounds **1a** and **1b**. Cell parameters were retrieved with SMART software[18] and refined with SAINT software[19] on all observed reflection ($I > 10\sigma(I)$). Data reduction was performed with SAINT, which corrects for Lorentz and polarization effects. An empirical absorption correction was applied for **1a** and **1b**. For compounds **2a** and **2b**, data were collected at 293 K on a P4 diffractometer using graphite monochromated Mo Kα radiation (λ = 0.71073Å), and were corrected for Lorentzian, polarization, and Ψ−scan absorption effects. All structures were solved by the use of direct methods, and refinement was performed by the least-squares methods on F^2 with the SHELXL-97 package,[20] incorporated in SHELXTL/PC V5.10.[21] Selected crystal data for the compounds (**1a**−**2b**) are summarized in Table 1.

1a. Crystals suitable for X-ray diffraction were grown from CH_2Cl_2 layered with hexane. A colorless crystal (0.52 × 0.40 × 0.26 mm^3) was mounted in the manner described above, and data were collected. A total of 10839 reflections were collected, of which 4104 were unique (R_{int} = 0.0264) and 2815 were observed with $I > 2\sigma(I)$. Hydrogen atoms were added to their idealized positions. The final cycle of the full-matrix least-squares refinement was based on 2815 observed reflections, and 211 parameters, and converged with unweighted and weighted agreement factors of R1 = 0.0476 and wR2 = 0.1094, respectively. The largest residual peak and hole are 0.919 e/Å^3 and −0.696 e/Å^3.

Table 1. Selected Crystallographic Data for $Ag_8(\mu_8\text{-}X)[Se_2P(OR)_2]_6(PF_6)$ (R= Et, X = Cl, **1a**, X = Br, **1b**; R= Pr, X = Cl, **2a**, X = Br, **2b**)

	1a	**1b**·1/2H$_2$O	**2a**	**2b**
formula	$C_{24}H_{60}ClAg_8F_6O_{12}P_7Se_{12}$	$C_{24}H_{61}BrAg_8F_6O_{12.5}P_7Se_{12}$	$C_{36}H_{84}ClAg_8F_6O_{12}P_7Se_{12}$	$C_{36}H_{84}BrAg_8F_6O_{12}P_7Se_{12}$
fw	2717.44	2770.91	2885.75	2930.21
space group	$R\bar{3}c$	$R\bar{3}c$	$R\bar{3}$	$R\bar{3}$
a, Å	18.078(2)	18.046(1)	22.053(2)	22.145(2)
b, Å	18.078(2)	18.046(1)	22.053(2)	22.145(2)
c, Å	74.607(9)	75.366(12)	14.150(3)	14.023(2)
α, deg	90	90	90	90
β, deg	90	90	90	90
γ, deg	120	120	120	120
V, Å^3	21117(3)	21256(4)	5960(1)	5955(1)
Z	12	12	3	3
ρ_{calcd}, g cm^{-3}	2.564	2.598	2.412	2.451
λ(Mo Kα), Å	0.71073	0.71073	0.71073	0.71073
μ, mm^{-1}	8.635	9.106	7.657	8.132
T, K	298(2)	298(2)	293(2)	293(2)
R1[a]	0.0476	0.0536	0.0521	0.0683
wR2[b]	0.1094	0.1350	0.1222	0.1572

[a] $R1 = \sum||F_o| - |F_c||/\sum|F_o|$. [b] $wR2 = \{\sum[w(F_o^2 - F_c^2)^2]/\sum[w(F_o^2)^2]\}^{1/2}$.

1b. Crystals suitable for X-ray diffraction were grown from CH_2Br_2 layered with hexane. A colorless crystal (0.55 × 0.50 × 0.40 mm^3) was mounted, and data were collected. A total of 14450 reflections were collected, of which 4126 were unique (R_{int} = 0.0287) and 2698 were observed with $I > 2\sigma(I)$. One of the ethoxy chains, O1−C3−C1, is found disordered. A model with fixed C−C (1.55 Å) and O−C (1.45 Å) distances was introduced. Hydrogen atoms were added. The final cycle of the full-matrix least-squares refinement was based on 2698 observed reflections, 2 restraints, and 212 parameters, and converged with unweighted and weighted agreement factors of R1 = 0.0536 and wR2 = 0.1366, respectively. The largest residual peak and hole are 0.897e/Å^3 and −1.451 e/Å^3.

2a. Crystals suitable for X-ray diffraction were grown from CH_2Cl_2 layered with hexane. A colorless crystal (0.40 × 0.38 × 0.30 mm^3) was mounted in the manner described above, and data were collected. A total of 2841 reflections were collected, of which 2252 were unique (R_{int} = 0.0882) and 1462 were observed with $I > 2\sigma(I)$. Hydrogen atoms were added to their idealized positions. The final cycle of the full-matrix least-squares refinement was based on 1462 observed reflections, and 125 parameters, and converged with unweighted and weighted agreement factors of R1 = 0.0521 and wR2 = 0.1222, respectively. The largest residual peak and hole are 0.475 e/Å^3 and −0.859 e/Å^3.

2b. Crystals suitable for X-ray diffraction were grown from CH_2Br_2 layered with hexane. A colorless crystal (0.40 × 0.15 × 0.10 mm^3) was mounted, and data were collected. A total of 2833 reflections were collected, of which 2251 were unique (R_{int} = 0.1488) and 1162 were observed with $I > 2\sigma(I)$. One of the propyl chains was found disordered. These disordered carbon atoms were treated in an equal population model. A model with fixed C−C (1.54 Å) and O−C (1.43 Å) distances was introduced. Hydrogen atoms were not added. The final cycle of the full-matrix least-squares refinement was based on 1162 observed reflections, 11 restraints, and 151 parameters, and converged with unweighted and weighted agreement factors of R1 = 0.0683 and wR2 = 0.1572, respectively. The largest residual peak and hole are 1.175 e/Å^3 and −1.226 e/Å^3.

(18) *SMART V4.043: Software for the CCD Detector System*; Bruker Analytical X-ray System: Madison, WI, 1995.
(19) *SAINT V4.043: Software for the CCD Detector System*; Bruker Analytical X-ray System: Madison, WI, 1995.
(20) Sheldrick, G. M. *SHELXL-97: Program for the Refinement of Crystal Structure*; University of Göttingen: Göttingen, Germany, 1997.
(21) *SHELXL 5.10 (PC verson): Program Library for Structure Solution and Molecular Graphics*; Bruker Analytical X-ray System: Madison, WI, 1998.

Scheme 1

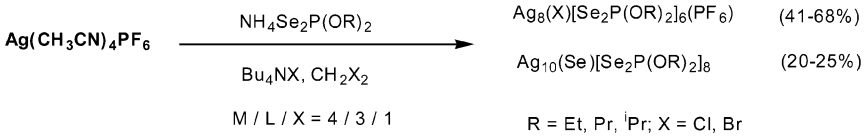

Results and Discussion

Synthesis and Characterization. Clusters $Ag_8(\mu_8\text{-Cl})[Se_2P(OEt)_2]_6(PF_6)$ (**1a**), $Ag_8(\mu_8\text{-Br})[Se_2P(OEt)_2]_6(PF_6)$ (**1b**), $Ag_8(\mu_8\text{-Cl})[Se_2P(OPr)_2]_6(PF_6)$ (**2a**), $Ag_8(\mu_8\text{-Br})[Se_2P(OPr)_2]_6(PF_6)$ (**2b**), $Ag_8(\mu_8\text{-Cl})[Se_2P(O^iPr)_2]_6(PF_6)$ (**3a**), and $Ag_8(\mu_8\text{-Br})[Se_2P(O^iPr)_2]_6(PF_6)$ (**3b**) were synthesized (Scheme 1) from the reaction of $[Ag(CH_3CN)_4](PF_6)$, $(NH_4)[Se_2P(OR)_2]$ (R= Et, Pr, ^{i}Pr), and Bu_4NX (X = Cl, Br) in a molar ratio of 4:3:1 in CH_2X_2 at 0 °C. The yields of the isolated product were 55%, 61%, 41%, 51%, 68%, and 65% for **1a**−**3b**, respectively, along with ∼20−25% $Ag_{10}(\mu_{10}\text{−Se})[Se_2P(OR)_2]_8$, which is known to form in the absence of halide ions.[17b]

Compounds **1a**−**3b** are well characterized by elemental analysis, FAB-MS, and ^{1}H and ^{31}P NMR spectroscopy. Elemental analyses of the compounds are in good agreement with the molecular formulation of clusters **1a**−**3b**. Positive fast-atom bombardment mass spectra (FAB-MS) of **1a**−**3b** in nitrobenzyl alcohol show the molecular ion peaks $[M - PF_6]^+$. The observed *m*/*z* peaks in the positive FAB mass spectra are 2573.2 for **1a** (M_{calc} = 2572.5), 2617.3 for **1b** (M_{calc} = 2616.9), 2740.9 for **2a** (M_{calc} = 2740.8), 2786.9 for **2b** (M_{calc} = 2785.3), 2742.3 for **3a** (M_{calc} = 2740.8), and 2787.0 for **3b** (M_{calc} = 2785.3), providing further evidence in support of the structural assignment for **1a**−**3b**. ^{31}P {^{1}H} NMR spectra of **1a**−**3b** display a singlet at δ 82.3, 81.5, 82.9, 81.7, 76.3, and 75.8 ppm with a set of satellites (J_{PSe} = 661, 664, 652, 652, 656, and 656 Hz, respectively), whereas the free ligands $NH_4[Se_2P(OR)_2]$ show a singlet at δ 88.0, 88.0, and 82.0 ppm (J_{PSe} = 720) with their respective ethyl, propyl, and isopropyl derivatives. The ∼5−6 ppm chemical shift from free dsep ligands to clusters (**1a**−**3b**) indicates the formation of clusters. ^{1}H NMR spectra exhibit chemical shifts at δ 1.39 and 4.17 ppm for the CH_2CH_3 group of the dsep ligand in **1a** and **1b**, 0.98−0.99, 1.74−1.77, and 4.05 ppm for the $CH_2CH_2CH_3$ group of the dsep in **2a** and **2b**, and 1.36−1.40 and 4.78−4.86 ppm for the $CH(CH_3)_2$ group of dsep in **3a** and **3b**. These NMR data suggest that all the dsep ligands are equivalent in solution and the geometry of the compounds **1a**−**3b** remains the same both in solid and in solution phase.

Crystal Structures. Four clusters **1a**−**2b** have been characterized by the single-crystal X-ray diffraction technique. The general structure feature consists of a discrete cationic cluster in which eight silver ions are linked by six face-capped diselenophosphate ligands and a central μ_8-Cl or μ_8-Br ion with a noncoordinating PF_6^- anion. Selected bond lengths and angles for **1a**, **1b**, **2a**, and **2b** are given in Tables 2, 3, 4, and 5, respectively. Eight silver atoms are arranged at the corner of the slightly distorted cube. Each selenium atom of the dsep ligand bridges two silver atoms; therefore, the dsep ligand exhibits a tetrametallic tetraconnective (μ_2, μ_2) coordination pattern[22] and each occupies a square face of the cube. Each silver atom is coordinated by three selenium atoms of three different ligands. In addition to the trigonal planar geometry around the silver atom, there is a bonding interaction to the central halide ion. The coordination geometry around the chloride or bromide ion is close to cubic although some irregular Ag−X distances are observed.

Compound **1a** is crystallized in the trigonal space group $R\bar{3}c$. Restricted by the crystallographic symmetry that is the

Table 2. Selected Bond Distances (Å) and Angles (deg) for $Ag_8(\mu_8\text{-Cl})[Se_2P(OEt)_2]_6(PF_6)$, **1a**, with Estimated Standard Deviations in Parentheses

Ag(1)−Cl(1)	2.917(3)	Ag(2A)−Ag(4)−Ag(2)	88.17(4)
Ag(2)−Cl(1))	2.809(1)	Se(2A)−Ag(1)−Se(2)	119.16(1)
Ag(4)−Cl(1)	2.923(4)	Se(1)−Ag(2)−Se(3B)	120.81(5)
Ag(3)−Cl(1)	2.978(1)	Se(1)−Ag(2)−Se(4)	115.44(5)
Ag(1)−Se(2A)	2.600(1)	Se(3B)−Ag(2)−Se(4)	116.16(5)
Ag(2)−Se(1)	2.613(1)	Se(3)−Ag(3)−Se(2A)	122.94(5)
Ag(2)−Se(3B)	2.618(1)	Se(3)−Ag(3)−Se(1)	118.60(5)
Ag(2)−Se(4)	2.635(1)	Se(2A)−Ag(3)−Se(1)	116.29(5)
Ag(3)−Se(3)	2.592(1)	Se(2A)−Ag(1)−Cl(1)	95.30(3)
Ag(3)−Se(2A)	2.607(1)	Se(1)−Ag(2)−Cl(1)	97.00(6)
Ag(3)−Se(1)	2.614(1)	Se(3B)−Ag(2)−Cl(1)	101.66(4)
Ag(4)−Se(4)	2.588(1)	Se(4)−Ag(2)−Cl(1)	99.00(6)
Ag(2)−Ag(3B)	3.222(1)	Se(1)−Ag(2)−Ag(3B)	97.05(4)
Ag(2)−Ag(4)	3.281(1)	Se(3B)−Ag(2)−Ag(3B)	51.43(3)
P−Se (av)	2.159	Se(4)−Ag(2)−Ag(3B)	143.40(4)
Se···Se (av)	3.805	Se(1)−Ag(2)−Ag(4)	139.15(4)
Se−P−Se (av)	123.64	Se(3B)−Ag(2)−Ag(4)	96.60(4)
Ag(2)−Se(1)−Ag(3)	81.46(4)	Se(4)−Ag(2)−Ag(4)	50.45(4)
Ag(1)−Se(2)−Ag(3B)	84.16(4)	Ag(2A)−Cl(1)−Ag(2)	108.75(6)
Ag(3)−Se(3)−Ag(2A)	76.40(4)	Ag(2A)−Cl(1)−Ag(1)	110.19(6)
Ag(4)−Se(4)−Ag(2)	77.82(2)	Ag(2A)−Cl(1)−Ag(4)	69.81(6)
Ag(3B)−Ag(2)−Ag(4)	94.02(3)	Ag(1)−Cl(1)−Ag(4)	180.0

Table 3. Selected Bond Distances (Å) and Angles (deg) for $Ag_8(\mu_8\text{-Br})[Se_2P(OEt)_2]_6(PF_6)$, **1b**, with Estimated Standard Deviations in Parentheses

Ag(1)−Br(1)	2.962(2)	Ag(2B)−Ag(4)−Ag(2A)	88.68(4)
Ag(2)−Br(1))	2.865(1)	Se(2B)−Ag(1)−Se(2A)	119.51(1)
Ag(3)−Br(1)	3.012(1)	Se(1A)−Ag(2)−Se(3A)	121.79(6)
Ag(4)−Br(1)	2.963(3)	Se(1A)−Ag(2)−Se(4)	115.83(6)
Ag(1)−Se(2A)	2.601(1)	Se(3A)−Ag(2)−Se(4)	116.20(6)
Ag(2)−Se(4)	2.639(2)	Se(3)−Ag(3)−Se(1A)	118.65 (5)
Ag(2)−Se(3A)	2.619(2)	Se(3)−Ag(3)−Se(2)	123.27(6)
Ag(2)−Se(1A)	2.615(2)	Se(2)−Ag(3)−Se(1A)	116.46(5)
Ag(3)−Se(3)	2.595(2)	Se(2)−Ag(1)−Br(1)	94.04(4)
Ag(3)−Se(1A)	2.620(2)	Se(1A)−Ag(2)−Br(1)	95.98(5)
Ag(3)−Se(2)	2.613(2)	Se(3A)−Ag(2)−Br(1)	100.61(4)
Ag(4)−Se(4)	2.596(2)	Se(4)−Ag(2)−Br(1)	98.34(5)
Ag(2)−Ag(3A)	3.269(1)	Se(1A)−Ag(2)−Ag(3A)	96.86(5)
Ag(2)−Ag(4)	3.328(2)	Se(3A)−Ag(2)−Ag(3A)	50.85(4)
P−Se (av)	2.159	Se(4)−Ag(2)−Ag(3A)	142.49(5)
Se···Se (av)	3.814	Se(1A)−Ag(2)−Ag(4)	138.25(5)
Se−P−Se (av)	124.07	Se(3A)−Ag(2)−Ag(4)	95.79(4)
Ag(2B)−Se(1)−Ag(3B)	82.69(5)	Se(4)−Ag(2)−Ag(4)	49.96(4)
Ag(1)−Se(2)−Ag(3)	85.79(5)	Ag(2)−Br(1)−Ag(4)	69.64(4)
Ag(3)−Se(3)−Ag(2B)	77.64(4)	Ag(2B)−Br(1)−Ag(3B)	72.04(3)
Ag(4)−Se(4)−Ag(2)	78.94(5)	Ag(2A)−Br(1)−Ag(3B)	67.53(3)
Ag(3A)−Ag(2)−Ag(4)	93.50(4)	Ag(1)−Br(1)−Ag(3B)	72.90(4)

(22) Haiduc, I.; Sowerby, D. B.; Lu, S.-F. *Polyhedron* **1995**, *14*, 3389.

Table 4. Selected Bond Distances (Å) and Angles (deg) for $Ag_8(\mu_8\text{-Cl})[Se_2P(OPr)_2]_6(PF_6)$, **2a**, with Estimated Standard Deviations in Parentheses

Ag(1)−Cl(1)	2.853(1)	Se(2A)−Ag(1)−Cl(1)	98.22(4)
Ag(1)−Se(1)	2.600(1)	Se(2)−Ag(1)−Cl(1)	98.17(4)
Ag(1)−Se(2A)	2.608(1)	Cl(1)−Ag(1)−Ag(1A)	54.81(1)
Ag(1)−Se(2)	2.611(1)	Se(1)−Ag(1)−Se(2A)	118.63(5)
Ag(2)−Se(1)	2.607(1)	Se(1)−Ag(1)−Se(2)	117.18(5)
Ag(1)−Ag(1A)	3.288(1)	Se(2A)−Ag(1)−Se(2)	118.39(4)
P−Se (av)	2.156	Se(1)−Ag(2)−Se(1C)	119.60(1)
Se···Se	3.809	Se(1)−Ag(1)−Ag(1A)	140.48(4)
Se(2B)−P(1)−Se(1)	123.88(13)	Se(2A)−Ag(1)−Ag(1A)	50.97(3)
Ag(1)−Se(1)−Ag(2)	81.53(4)	Se(2)−Ag(1)−Ag(1A)	96.38(5)
Ag(1B)−Se(2)−Ag(1)	78.11(4)	Se(1)−Ag(1)−Ag(1B)	95.09(4)
P(1)−Se(1)−Ag(1)	106.65(9)	Se(2A)−Ag(1)−Ag(1B)	140.67(4)
P(1)−Se(1)−Ag(2)	106.88(9)	Ag(1A)−Cl(1)−Ag(1C)	180.0
P(1A)−Se(2)−Ag(1B)	106.01(8)	Ag(1A)−Cl(1)−Ag(1E)	109.63(2)
P(1A)−Se(2)−Ag(1)	105.30(9)	Ag(1C)−Cl(1)−Ag(1E)	70.37(2)
Ag(1A)−Ag(1)−Ag(1B)	90.33(4)	Ag(1A)−Cl(1)−Ag(1D)	70.38(2)
Se(1)−Ag(1)−Cl(1)	97.80(3)	Ag(1C)−Cl(1)−Ag(1D)	109.62(2)

Table 5. Selected Bond Distances (Å) and Angles (deg) for $Ag_8(\mu_8\text{-Br})[Se_2P(OPr)_2]_6(PF_6)$, **2b**, with Estimated Standard Deviations in Parentheses

Ag(1)−Br(1)	2.911(1)	Se(2)−Ag(1)−Br(1)	97.30(5)
Ag(2)−Br(1)	3.072(3)	Se(1B)−Ag(2)−Br(1)	92.62(6)
Ag(1)−Se(1)	2.608(2)	Br(1)−Ag(1)−Ag(1A)	54.88(1)
Ag(1)−Se(2A)	2.615(2)	Se(1)−Ag(1)−Se(2A)	118.87(7)
Ag(1)−Se(2)	2.617(2)	Se(1)−Ag(1)−Se(2)	117.53(7)
Ag(1)−Ag(1B)	3.349(2)	Se(2A)−Ag(1)−Se(2)	119.12(6)
P−Se (av)	2.157	Se(1B)−Ag(2)−Se(1A)	119.79(1)
Se····Se	3.818	Se(1)−Ag(1)−Ag(1B)	94.22(5)
Se(2B)−P(1)−Se(1)	124.5(2)	Se(2A)−Ag(1)−Ag(1B)	140.35(7)
Ag(1)−Se(1)−Ag(2C)	83.25(7)	Se(2)−Ag(1)−Ag(1B)	50.17(5)
Ag(1B)−Se(2)−Ag(1)	79.61(6)	Se(1)−Ag(1)−Ag(1A)	139.53(6)
P(1)−Se(1)−Ag(1)	106.69(14)	Se(2A)−Ag(1)−Ag(1A)	50.22(5)
P(1)−Se(1)−Ag(2C)	107.38(13)	Se(2)−Ag(1)−Ag(1A)	96.07(7)
P(1A)−Se(2)−Ag(1B)	106.50(12)	Ag(1B)−Br(1)−Ag(1)	70.24(3)
P(1A)−Se(2)−Ag(1)	104.84(14)	Ag(1B)−Br(1)−Ag(1C)	109.76(3)
Ag(1B)−Ag(1)−Ag(1A)	90.61(5)	Ag(1)−Br(1)−Ag(1C)	180.0
Se(1)−Ag(1)−Br(1)	96.59(5)	Ag(1B)−Br(1)−Ag(2C)	109.18(3)
Se(2A)−Ag(1)−Br(1)	97.35(5)	Ag(1)−Br(1)−Ag(2C)	70.82(3)

absence of inversion center, the Cl(1) atom does not locate exactly in the center of the cube (Figure 1). Thus, four kinds of Ag−Cl distances are revealed and range from 2.809 to 2.978 Å. These distances are significantly shorter than those found in clusters $[Ni^{II}_6Ag^{I}_8(\text{D-pen})_{12}Cl]^{5-}$ and $[Ag_{14}(C{\equiv}C^{t}\text{-}Bu)_{12}Cl]^{+}$ which lie in the range 2.897−3.136 and 3.116−3.297 Å, respectively. The average Ag−Ag distance is 3.351 Å, shorter than 3.477 Å in $[Ni^{II}_6Ag^{I}_8(\text{D-pen})_{12}Cl]$,$^{5-}$ but longer than 3.269 Å in $Ag_8(\mu_8\text{-Se})[Se_2P(O^{i}Pr)_2]_6$[23] clusters. The average Ag−Se bond distance is 2.608 Å, comparable to a Ag-μ_2−Se bond distance, 2.599 Å, in $Ag_8(\mu_8\text{-Se})[Se_2P(O^{i}\text{-}Pr)_2]_6$.[23] The average P−Se distance is 2.159 Å. The average Se···Se bite distance is 3.805 Å, comparable to 3.808 Å in $Cu_8(\mu_8\text{-Cl})[Se_2P(OEt)_2]_6(PF_6)$.[10b] The average Se−P−Se angle is 123.64°. The Se−Ag−Se angle ranges from 115.44° to 120.81°. The Ag−Cl−Ag angles lie in the range 67.6−72.6° whereas in the perfect cube this angle is 70.53°.[9e]

Cluster **2a** crystallizes in the trigonal space group $R\bar{3}$. Two silver atoms are located in the asymmetric unit with the C_3 rotational axis through Ag2 and Cl(1) atoms (Figure 2). The average Ag−Ag distance is 3.344 Å which is longer than 2.965 Å in $[Ag_{14}(C{\equiv}C^{t}Bu)_{12}Cl]^{+}$ [13b] but comparable to **1a**.

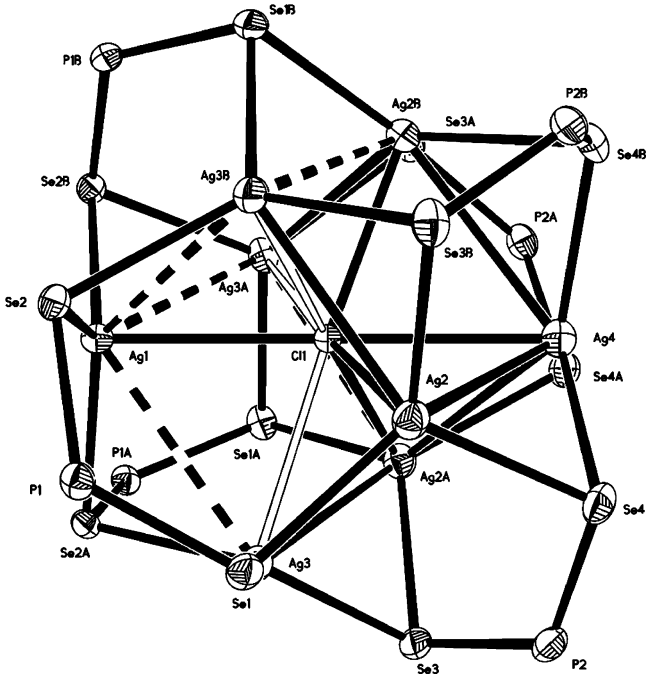

Figure 1. Thermal ellipsoid drawing (50% probability level) of the cation of cluster $Ag_8(\mu_8\text{-Cl})[Se_2P(OEt)_2]_6(PF_6)$ showing the atom-numbering scheme. The ethoxyl groups are omitted for clarity.

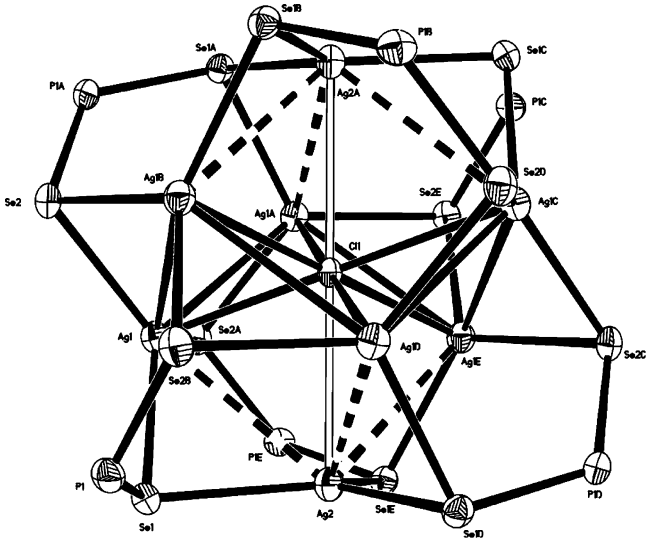

Figure 2. Thermal ellipsoid drawing (50% probability level) of the cation of cluster $Ag_8(\mu_8\text{-Cl})[Se_2P(OPr)_2]_6(PF_6)$ with the atom-labeling scheme. The propoxyl groups are omitted for clarity.

In **2a**, six Ag−Cl bonds have the same distance, 2.853 Å, with two longer Ag−Cl bonds along the C_3 having a distance of 3.020 Å. The Ag−Se distances range between 2.600 and 2.611 Å. The P−Se distances are in the range 2.151−2.165 Å with an average of 2.156 Å. The Se···Se bite distance is 3.809 Å, and the Se−P−Se angle is 123.88°. The Se−Ag−Se angles range from 117.17° to 119.60°. The average of Ag−Cl−Ag angles is 70.55°.

All Ag−Ag and Ag−Cl distances in clusters **1a** and **2a** appear approximately 0.1 Å shorter than those in the mixed-metal cluster, $[Ni^{II}_6Ag^{I}_8(\text{D-pen})_{12}Cl]^{5-}$, where the central core, Ag_8Cl, is ligated by the S-atoms of the D-penicillamine. This reveals the metal core contraction for the selenium donor ligands. It has been identified previously in two types of close

(23) Liu, C. W.; Shang, I.-J.; Wang, J.-C.; Keng, T.-C. *Chem. Commun.* **1999**, 995.

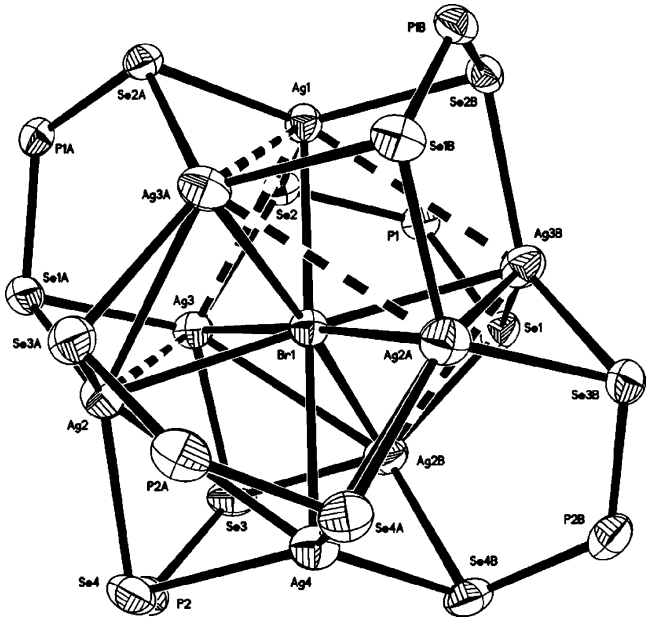

Figure 3. Thermal ellipsoid drawing (50% probability level) of the cation of cluster $Ag_8(\mu_8\text{-Br})[Se_2P(OEt)_2]_6(PF_6)$ showing the atom-numbering scheme. The ethoxyl groups are omitted for clarity.

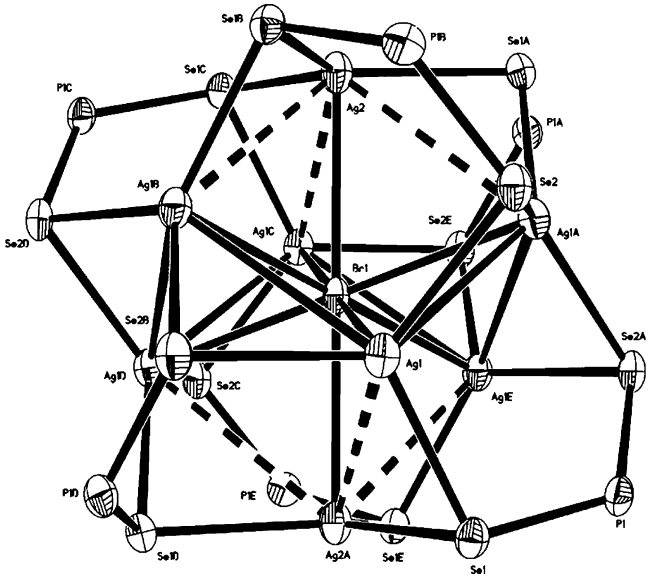

Figure 4. Thermal ellipsoid drawing (50% probability level) of the cation of cluster $Ag_8(\mu_8\text{-Br})[Se_2P(OPr)_2]_6(PF_6)$ with the atom-labeling scheme. The propoxyl groups are omitted for clarity.

shell ion-centered cuboidal structure of copper connected by either S- or Se-containing ligands.[24] It was suggested that the bridging ligands are responsible for the observed Cu···Cu contacts and copper atoms carry more positive charge in the presence of the more electronegative S-containing ligands; therefore, there are greater Cu···Cu separations due to the existing moderate Cu···Cu repulsion. It seems that the charge argument in the copper systems can also be utilized to explain the contraction phenomenon observed in the chloride-centered cuboidal silver clusters. Certainly, it will be of great interest to isolate the discrete, chloride-centered Ag_8 cluster ligated entirely by the sulfur atoms such as the hitherto unknown molecule $Ag_8(Cl)[S_2P(OR)_2]_6(PF_6)$ and to make a detailed structural comparison.

Compound **1b** crystallized in rhombohedral space group $R\bar{3}c$. The 3-fold rotational axis passes through the Ag(1), Br(1), and Ag(4) atoms (Figure 3). Because of a lack of inversion center, the Br(1) atom does not exactly locate in the center of the cube although the distances between Br(1) and two silver atoms on the C_3 are almost identical, 2.962 and 2.963 Å. The rest of the Ag−Br distances are in the range 2.865−3.012 Å, significantly shorter than observed lengths 3.148−3.313 Å in $[Ag_{14}(C{\equiv}C^tBu)_{12}Br]^+$.[13a] The Ag−Ag distances are in the range 3.269−3.549 Å, slightly longer than 3.222−3.490 Å in chloride-centered Ag_8 cubes. The Ag−Se distances vary from 2.595 to 2.639 Å and are comparable to **1a** and **2a**. The P−Se distances range from 2.152 to 2.170 Å. The ligand bite diatances averaged 3.814 Å which slightly longer than 3.784 Å in the selenium-centered copper cube.[25] The Se−Ag−Se angles range from 116.19° to 123.26°. The Ag−Br−Ag angles fall in the range 67.53−72.89°, close to the value for the perfect cube, 70.53°.

Compound **2b** crystallizes in the trigonal space group $R\bar{3}$. Two silver atoms are located in the asymmetric unit with the C_3 rotational axis through Ag(2) and Br(1) atoms (Figure 4). The average Ag−Ag distance is 3.409 Å which is longer than the observed length 2.984 Å in $[Ag_{14}(C{\equiv}C^tBu)_{12}Br]^+$.[13b] Six Ag−Br bonds have the same distance, 2.911 Å, with two longer Ag−Br bonds along the C_3 axis having a distance of 3.072 Å, but shorter than 3.148−3.313 Å found in $[Ag_{14}(C{\equiv}C^tBu)_{12}Br]^+$.[13] The Ag−Se distances vary from 2.608 to 2.617 Å. The P−Se distances range from 2.154 to 2.161 Å. The Se···Se bite distance is 3.818 Å, and the Se−P−Se angle is 124.5°. The Se−Ag−Se angles range from 117.53° to 119.79°. The average Ag−Br−Ag angle is 70.53°.

Four of the six clusters are structurally characterized. They crystallized in the same crystal system, trigonal, but in different space groups; the ethyl derivatives are $R\bar{3}c$, but $R\bar{3}$ for the *n*-propyl groups. These are exactly the same as their copper analogues.[10c] Thus, the remaining two, **3a** and **3b**, which have not been characterized structurally to date, may crystallize in the monoclinic space group, $C2/c$, as their copper counterparts do.

Molecular Orbital Calculations. In the preceding sections, we have described the characterization of several newly synthesized halide-centered cubic silver clusters. In this section, we report our results of the molecular orbital calculations[26] at the B3LYP level of density functional theory with the hope of providing theoretical insight into the nature of Ag−μ_8-X (X = Cl, Br) bonding interactions. Table 6 gives the results of natural bond orbital (NBO) analyses.[27] For comparison, Table 6 also gives the results calculated for $Ag_8(\mu_8\text{-Se})\{Se_2P(O^iPr)_2\}_6$[23] and $Cu_8(\mu_8\text{-Se})\{Se_2P(OPr)_2\}_6$.[28]

We can see from Table 6 that small Wiberg bond indices (also called bond orders)[29] were calculated for the Ag−μ_8-X bonds, indicating that the Ag−μ_8-X bonding interactions are not strong. In an early paper, we formally assigned a half bond between each Cu(I) and the central μ_8-Se for various

(24) Liu, C. W.; Hung, C.-M.; Santra, B. K.; Wang, J.-C.; Kao, H.-M.; Lin, Z. *Inorg. Chem.* **2003**, *42*, 8551.
(25) Liu, C. W.; Chen, H.-C.; Wang, J.-C.; Keng, T.-C. *Chem. Commun.* **1998**, 1831.

Table 6. Results of Natural Bond Order and Population Analyses[a]

cluster	Wiberg bond index		natural charge			HOMO−LUMO gap (ev)
	M−μ_8-X	M−Se (terminal)	M	μ_8-X	Se (terminal)	
$[Ag_8(\mu_8\text{-Cl})\{Se_2P(OPr)_2\}_6]^+$ [b]	0.05	0.21	+0.61	−0.75	−0.56	4.31
$[Ag_8(\mu_8\text{-Br})\{Se_2P(OPr)_2\}_6]^+$ [b]	0.05	0.21	+0.60	−0.74	−0.54	4.24
$Ag_8(\mu_8\text{-Se})\{Se_2P(O^iPr)_2\}_6$ [b]	0.09	0.19	+0.62	−1.48	−0.56	2.99
$Cu_8(\mu_8\text{-Se})\{Se_2P(OPr)_2\}_6$ [c]	0.09	0.19	+0.63	−1.49	−0.56	3.15

[a] M = Ag or Cu; X = Cl, Br, or Se. [b] The alkyl groups were replaced with hydrogen atoms in the model calculations. [c] Cited from ref 24.

Se-centered Cu_8 cubic clusters because there are only four bonding molecular orbitals, which are derived from the interactions between the four valence orbitals of the central μ_8-Se and four symmetry-adapted combinations from the eight Cu metals, for the eight Cu(I)−μ_8-Se bonds.[24] It is expected that the same bonding picture can be qualitatively used to describe the Ag(I)−μ_8-X interactions here.

Despite the similarity in the bonding pictures, we found that the bond indices calculated for Ag−μ_8-X are much smaller than those calculated for Ag−μ_8-Se and Cu−μ_8-Se. The difference can be conveniently related to their different electronegativities. Both Cl and Br are more electronegative than Se. Therefore, the Ag−μ_8-X bonds are expected to be more ionic while the Ag−μ_8-Se and Cu−μ_8-Se bonds are more covalent. Indeed, the bond distances between Ag and μ_8-X (Ag−μ_8-Cl, 2.81−3.02 Å; Ag−μ_8-Br, 2.91−3.07 Å) are approximately equal to or slightly longer than the sums of their ionic radii (Ag−Cl, 2.81 Å; Ag−Br, 2.96 Å) while the bond distances between Ag or Cu and μ_8-Se (Ag-μ_8-Se, 2.71−2.87 Å; Cu-μ_8-Se, 2.50−2.52 Å) are shorter than the sums of their ionic radii (Ag−Se, 2.98 Å; Cu−Se, 2.58 Å).[30]

The calculations also show that the bond indices for Ag−μ_8-Cl and Ag−μ_8-Br are the same. Structurally, one can see that the magnitude of the $Ag_8(\mu_8$-X) core expansion (ca. 0.10 Å in radius) from $Ag_8(\mu_8$-Cl) to $Ag_8(\mu_8$-Br) is smaller than the increase (0.15 Å) in size from Cl^- [$r(Cl^-)$ = 1.67 Å] to Br^- [$r(Br^-)$ = 1.82 Å].[30] Therefore, we expected that the covalent interaction between Ag and μ_8-Br is stronger than that between Ag and μ_8-Cl. The magnitude of the $M_8(\mu_8$-X) core expansion from $Cu_8(\mu_8$-Se) to $Ag_8(\mu_8$-Se) is in the range 0.21−0.35 Å in radius, which is also smaller than the increase (0.40 Å) in the size from Cu^+ [$r(Cu^+)$ = 0.74 Å] to Ag^+ [$r(Ag^+)$ = 1.14 Å]. Again, the Ag is expected to have more covalent interactions with the central Se.

The HOMO−LUMO gaps of the two halide-centered clusters are close to each other (Table 6). Unlike the two Se-centered clusters having their HOMOs mainly composed of the three p orbitals from the central Se,[24] the two halide-centered clusters have their HOMOs mainly composed of the p orbitals from Se of the $Se_2P(OR)_2^-$ ligands. The three p orbitals of the central halide lie lower in energy in the orbital spectra due to its greater electronegativity in comparison to Se. As a result, the two halide-centered clusters have larger HOMO−LUMO gaps than the two Se-centered clusters.

The LUMOs calculated for all the clusters have P−Se σ^* antibonding characters mixed with metal's orbitals. Therefore, it is expected that the HOMO−LUMO transitions in these clusters correspond to ligand-to-ligand and ligand-to-metal charge transfers.

Acknowledgment. We thank the National Science Council of Taiwan (NSC 92-2113-M-033-012) for the financial support.

Supporting Information Available: X-ray crystallographic file in CIF format for compounds **1a**, **1b**, **2a**, and **2b**. This material is available free of charge via the Internet at http://pubs.acs.org.

IC049533P

(26) Density functional calculations at the B3LYP level were performed on the model clusters $[Ag_8(\mu_8\text{-X})\{Se_2P(OH)_2\}_6]^+$ (X = Cl, Br) based on the experimentally determined structures. The basis set used for O and H atoms was 6-31G while an effective core potential with a LanL2DZ basis set was employed for Ag, P, Cl, Br, and Se. The DFT calculations were performed with the use of the Gaussian 98 package: Frisch, M. J.; Trucks, G. W.; Schlegel, H. B.; Scuseria, G. E.; Robb, M. A.; Cheeseman, J. R.; Zakrzewski, V. G.; Montgomery, J. A., Jr.; Stratmann, R. E.; Burant, J. C.; Dapprich, S.; Millam, J. M.; Daniels, A. D.; Kudin, K. N.; Strain, M. C.; Farkas, O.; Tomasi, J.; Barone, V.; Cossi, M.; Cammi, R.; Mennucci, B.; Pomelli, C.; Adamo, C.; Clifford, S.; Ochterski, J.; Petersson, G. A.; Ayala, P. Y.; Cui, Q.; Morokuma, K.; Malick, D. K.; Rabuck, A. D.; Raghavachari, K.; Foresman, J. B.; Cioslowski, J.; Ortiz, J. V.; Stefanov, B. B.; Liu, G.; Liashenko, A.; Piskorz, P.; Komaromi, I.; Gomperts, R.; Martin, R. L.; Fox, D. J.; Keith, T.; Al-Laham, M. A.; Peng, C. Y.; Nanayakkara, A.; Gonzalez, C.; Challacombe, M.; Gill, P. M. W.; Johnson, B. G.; Chen, W.; Wong, M. W.; Andres, J. L.; Head-Gordon, M.; Replogle, E. S.; Pople, J. A. *Gaussian 98*, revision A.9; Gaussian, Inc.: Pittsburgh, PA, 1998.

(27) Reed, A.; Curtiss, L. A.; Weinhold, F. *Chem. Rev.* **1988**, *88*, 899.

(28) Liu, C. W.; Hung, C.-M.; Wang, J.-C.; Keng, T.-C. *J. Chem. Soc., Dalton Trans*. **2002**, 3482.

(29) Wiberg, K. B. *Tetrahedron* **1968**, *24*, 1083. The Wiberg bond indices (bond orders) are a measure of bond strength.

(30) Shannon, R. D. *Acta Crystallogr*. **1976**, *A32*, 751.